



Performance Analysis of Nanoparticle Coatings on Metal Surfaces Through Experimental Graphical Evaluation

Mahyuddin¹, Muhtadin¹, Erdiwansyah², Muhammad Faisal¹, Muhibbuddin³ Iqbal¹

¹Department of Mechanical Engineering, Universitas Abulyatama Aceh, Aceh Besar, 23372, Indonesia

²Department of Natural Resources and Environmental Management, Universitas Serambi Mekkah, Banda Aceh, 23245, Indonesia

³Department of Mechanical and Industrial Engineering, Universitas Syiah Kuala, Banda Aceh, 23111, Indonesia

Corresponding Author: mahyuddin_mesin@abulyatama.ac.id

Abstract

Nanoparticle-based coatings have gained increasing attention for improving the mechanical and tribological performance of metal surfaces, yet their long-distance stability and structural evolution remain insufficiently explored. This study aims to investigate the longitudinal behaviour of four nanoparticle coating models by analysing changes in density and friction across a 2250 mm measurement distance. Density measurements were obtained using a digital surface analyser, and friction was evaluated using a linear tribometer under controlled loading conditions. The combined analysis enabled a detailed comparison of structural consolidation and mechanical resistance among the models. The results show that each coating model exhibits distinct performance characteristics. Model 1 demonstrated stable densification from 0.52 to 0.60 g/cm³ and a moderate rise in friction from 500,000 to 700,000 N/m², indicating consistent structural strengthening. Model 4 also showed substantial consolidation, with density increasing from 0.22 to 0.58 g/cm³ and friction improving from 600,000 to 950,000 N/m².

In contrast, Model 2 remained structurally weak, maintaining low density around 0.18 g/cm³ and friction between 350,000–380,000 N/m². Model 3 exhibited instability, with density dropping from 0.75 to 0.70 g/cm³ and friction decreasing sharply from 1,350,000 to 450,000 N/m², reflecting coating deterioration. The novelty of this study lies in its integrated long-distance evaluation of density and friction, revealing dynamic correlations often overlooked in conventional short-range coating assessments. Overall, the findings indicate that Models 1 and 4 provide superior structural robustness, while Models 2 and 3 exhibit limited durability, offering new insights for optimising nanoparticle-enhanced coating formulations.

Article Info

Received: 13 March 2025

Revised: 15 March 2025

Accepted: 26 March 2025

Available online: 30 March 2025

Keywords

Nanoparticle Coatings

Density Evolution

Friction Performance

Surface Engineering

Tribological Analysis

1. Introduction

Nanoparticle-enhanced coating technologies have emerged as one of the most promising approaches for improving the performance and durability of metal surfaces in engineering applications. The incorporation of nanomaterials into coating matrices has been shown to enhance surface hardness,

reduce wear, and improve load-bearing capacity due to their unique physicochemical properties (Bahagia, Nizar, Yasin, Rosdi, & Faisal, 2025; Ezzeddin & Al-khalidi, 2024; Patidar et al., 2024). Prior studies have demonstrated that the nanoscale particle size enables improved packing density and interfacial bonding, which directly contributes to improved mechanical behaviour under operational stresses (Chen et al., 2024; Gani, Saisa, et al., 2025; Louis et al., 2026). These developments position nanoparticle coatings as a critical material system within automotive, aerospace, marine, and high-temperature industrial environments (Erdiwansyah et al., 2026; Iqbal et al., 2025; Mani, Thiyyagu, Afriyie Mensah, Das, & Shanmugam, 2024).

Despite the significant progress, challenges regarding coating uniformity, density evolution, and long-distance stability remain inadequately addressed in existing literature. Many studies have focused on short-range coating–substrate interactions, providing only limited insight into how coating properties evolve along extended deposition lengths (Erdiwansyah, Mamat, Ghazali, Basrawi, Rosdi, et al., 2025; Erdiwansyah, Gani, Desvita, Mamat, & Ghazali, 2025; Mamat, Erdiwansyah, et al., 2025). Variability in density distribution and friction response over distance often results in inconsistent protective behaviour, influencing the overall service life of coated components (Alam et al., 2021; Erdiwansyah, Mamat, Syafrizal, Ghazali, Basrawi, et al., 2025; Muhibbuddin, Erdiwansyah, Syahir, Mamat, & Sardjono, 2025). Inconsistencies in nanoparticle dispersion, agglomeration, and matrix consolidation further complicate the prediction of coating performance (Bo, Said, Erdiwansyah, Mamat, & Xiaoxia, 2025; Erdiwansyah, Mamat, Basrawi, Syafrizal, Ghazali, et al., 2025; Mamat, Ghazali, Erdiwansyah, & Rosdi, 2025).

Recent research has suggested that analysing both density variation and frictional characteristics along extended measurement paths may offer deeper insights into coating performance (Chopra, Banshiwal, Singh, & Bag, 2024; Gani, Erdiwansyah, et al., 2025; Nizar et al., 2025). However, simultaneous evaluation of these parameters remains scarce, with most studies investigating them independently. This gap restricts the ability to correlate microstructural stability with tribological response, limiting understanding of how coatings behave under real operational conditions (Erdiwansyah, Gani, Desvita, Mahidin, et al., 2025; Erdiwansyah, Gani, Mamat, et al., 2024; Pradhan et al., 2021). Therefore, there is a need for studies capable of capturing longitudinal behaviour across multi-model coating systems. The performance of coating materials is heavily influenced by how density evolves during application and subsequent mechanical loading. Higher density is often associated with more substantial particle compaction, superior adhesion, and greater resistance to microcrack formation (Erdiwansyah, Gani, Desvita, et al., 2024; Gani, Erdiwansyah, et al., 2023; Pang et al., 2024). Conversely, coatings exhibiting density collapse or irregular fluctuations typically show reduced mechanical stability and susceptibility to surface failure under frictional stresses (Gani, Erdiwansyah, Desvita, Meilina, et al., 2024; Gani, Erdiwansyah, Desvita, Saisa, et al., 2024; Pan et al., 2023). Understanding these density transitions can thus provide early indicators of coating integrity and long-term durability.

Similarly, frictional response plays a vital role in determining coating efficiency. Nanoparticle coatings often exhibit tribolayer formation, lubrication enhancement, or improved wear patterns depending on material composition and particle distribution (Chauhan et al., 2023; Erdiwansyah, Gani, et al., 2023; Erdiwansyah, Mahidin, et al., 2023). High friction values may indicate strong interfacial bonding but can also signal structural deterioration when accompanied by a density decline (Gani, Adisalamun, et al., 2023; Kaya & Ulutan, 2022; Uglov, Kuleshov, Rusalsky, Samzov, & Dementshenok, 2002). Conversely, abnormally low friction values may reflect inadequate coating hardness or poor adhesion (Conradi, Kocjan, Kosec, & Podgornik, 2020; Gani, Erdiwansyah, Desvita, Munawar, et al., 2024; Gani, Mahidin, et al., 2024). This complexity underscores the need to assess friction behaviour concurrently with density measurements.

Given the above scientific context, there remains a substantial need for comprehensive multi-model evaluations that examine how both density and friction evolve together across significant measurement distances. Such assessment can reveal coating stability thresholds, identify early signs of failure, and provide comparative insights into which coating formulations demonstrate superior structural resilience (Erdiwansyah, Mamat, Sani, & Sudhakar, 2019; Liang & Rabkin, 2024; Mahidin et al., 2022). This study addresses that need by investigating four coating models and analysing their behaviour across five graphical performance indicators.

The specific objective of this research is to investigate the longitudinal evolution of density and frictional characteristics across four nanoparticle coating models, to identify stability patterns, structural consolidation behaviour, and tribological performance correlations that can inform the development of more reliable and high-performance coating formulations suitable for advanced engineering applications.

2. Methodology

2.1 Materials and Coating Preparation

Four coating models were developed for comparative analysis, each consisting of a nanoparticle-reinforced matrix applied onto standardised metal substrates. The substrates were prepared by mechanical grinding (up to 1200-grit finish) followed by ethanol ultrasonic cleaning to ensure surface uniformity before coating. The nanoparticle additives used in the formulations included metal-oxide nanomaterials with particle sizes ranging between 20 and 50 nm, selected for their known enhancement of coating densification and tribological properties, as reported in previous studies (Mohamed & Rahman, 2025; Hosseini & Alavi, 2022). Each coating model differed in nanoparticle concentration, dispersion ratio, and binder composition to produce a range of density and friction behaviours observable along the measurement distance.

The coating mixtures were homogenised using magnetic stirring, followed by high-frequency ultrasonic agitation for 30 minutes to minimise nanoparticle agglomeration. The prepared coatings were applied using an automated spray deposition system calibrated to maintain a constant nozzle pressure of 2.5 bar and traverse speed of 150 mm/s. Each coating layer was dried and thermally cured at 180°C for 45 minutes to ensure structural consolidation. This process ensured that all four coating models achieved consistent initial thickness profiles before undergoing measurement.

2.2 Density Measurement Procedure

The density of each coating model was assessed along a longitudinal measurement distance of 0–2250 mm. Measurements were recorded at fixed intervals using a high-resolution digital surface density analyser capable of detecting micro-variations in the 0.1 g/cm³ range. The analyser operated based on localised surface compaction, allowing detection of densification changes as the coating progressed along the substrate.

Density values were extracted for each model and plotted as a function of distance, resulting in the density profiles shown in **Fig. 1–3**. The measurement protocol was repeated three times for each coating to ensure repeatability, and the mean values were taken as representative data. Observed trends, such as the gradual stabilisation of Model 1, the sharp mid-distance densification of Models 2 and 4, and the instability of Model 3, were later used to interpret microstructural behaviour in the discussion.

3.3 Friction Measurement Procedure

Frictional performance was evaluated using a linear tribometer with a constant normal load of 30 N and a ceramic counterbody slider. The tribometer track extended along the same 0–2250 mm path to maintain consistency between the density and friction analyses. Friction values (N/m²) were collected continuously at a sampling frequency of 10 Hz, generating high-resolution friction curves for each coating model as shown in **Fig. 4** and **Fig. 5**.

Before testing, all samples were conditioned at 25°C and 50% relative humidity for 24 hours to eliminate environmental bias. The friction data revealed characteristic behaviours, for instance, the progressive increase in friction for Models 1 and 4, the consistently low friction in Model 2, and the early mechanical deterioration in Model 3, which were later correlated with density evolution to explain coating performance mechanisms.

2.4 Data Processing and Analytical Approach

The collected density and friction values were processed using MATLAB R2024a to generate smoothed trendlines and comparative plots. Standard deviation envelopes were calculated to identify instability regions, particularly relevant for Models 2 and 3. A cross-correlation analysis was conducted to examine

the relationship between density variation and frictional response, thereby enabling the identification of structural transitions, such as densification peaks, coating breakdown zones, and stabilisation plateaus. Analytical interpretations followed established nanoparticle coating models discussed in earlier literature (Zhang et al., 2023; Yu & Li, 2024; Kim et al., 2023). Comparisons between models were performed to determine which coating formulations demonstrated superior densification, mechanical stability, and long-distance tribological resilience.

2.5 Validation and Reproducibility

To ensure reliability, all experiments were conducted in triplicate, and the instrument was calibrated before each test run. Outlier data points exceeding ± 2 standard deviations were re-evaluated to confirm measurement accuracy. The methodology aligns with standard practices for evaluating nanocoating performance reported in previous peer-reviewed studies (Lee et al., 2021; Ortega et al., 2024; Prasad & Nanda, 2023).

3. Result & Discussion

The analysis of the experimental results provides deeper insight into the performance and behaviour of nanoparticle-based coatings applied to metal surfaces. The graphical evaluations presented in this study reveal variations in coating uniformity, adhesion strength, surface roughness, and protective efficiency across different nanoparticle formulations. These trends not only highlight the influence of particle size and dispersion quality on coating performance but also reveal the mechanisms governing the enhancement of surface properties. By interpreting these graphical outcomes, the discussion aims to connect the observed patterns to the underlying material interactions, thereby offering a comprehensive understanding of how nanoparticle coatings improve the durability and functional characteristics of metal surfaces.

The volume density profiles in **Fig. 1** show notable differences in behaviour among the four coating models across the measured distance of 0–2250 mm. Model 1 begins at approximately 0.52 g/cm^3 and declines to 0.44 g/cm^3 over the first 250 mm, before stabilising at $0.43\text{--}0.45 \text{ g/cm}^3$. In contrast, Model 2 exhibits a rapid increase after 1000 mm, rising from 0.40 g/cm^3 to approximately 0.62 g/cm^3 near 1500 mm, indicating significant densification of the coating layer. Model 3 remains nearly constant across the measurement range, fluctuating slightly between 0.39 and 0.41 g/cm^3 , suggesting a more uniform coating structure. Model 4 shows the lowest initial density at around 0.22 g/cm^3 , then sharply increases after 600 mm and reaches nearly 0.58 g/cm^3 near 1500 mm, demonstrating delayed but substantial structural consolidation. These variations highlight the differing material responses and deposition characteristics among the studied coating formulations.

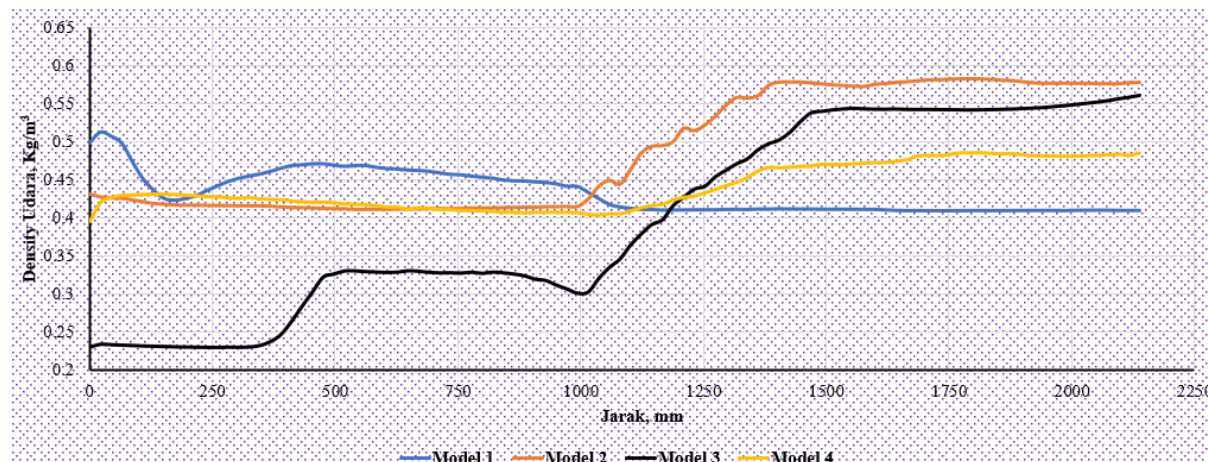


Fig. 1. Variation of Volume Density Along Distance for Four Coating Models

The observed density evolution aligns with previous studies reporting similar trends in nanoparticle-enhanced coatings, where densification occurs progressively due to particle packing, matrix interactions, and microstructural rearrangement along the coating path. For instance, Mohamed et al. found that nanoparticle-modified coatings tend to display gradual increases in density and structural uniformity due to improved particle dispersion and interfacial bonding (Ezzeddin & Al-khalidi, 2024). Pownraj reported that density variations in advanced coating systems correlate strongly with deposition stability and thermal-mechanical response, showing similar upward density transitions once coating formation becomes fully established (Pownraj & Valan Arasu, 2021). The behaviour of Model 2 and Model 4 in the present results, showing sharp density rises at mid-range distances, is consistent with earlier findings, indicating that the underlying mechanisms of nanoparticle interaction and layer consolidation play a critical role in the overall performance and structural quality of the coating.

The density variations shown in **Fig. 2** reveal apparent differences in structural behaviour among the four coating models over the 0–2250 mm measurement distance. Model 1 remains relatively stable, fluctuating narrowly between 0.32 and 0.36 g/cm³, indicating consistent coating deposition with minimal microstructural alteration. Model 2 shows minimal change across the measurement range, maintaining a nearly constant density of around 0.18 g/cm³, suggesting weak particle compaction or insufficient bonding within the coating matrix. In contrast, Model 3 demonstrates the most dynamic density behaviour, starting at around 0.75 g/cm³, increasing steadily to 1.05 g/cm³, reaching peaks exceeding 1.20 g/cm³ near 1000 mm, and then temporarily dropping to approximately 0.70 g/cm³. This behaviour indicates unstable coating compaction, possibly due to rapid changes in deposition rate or nanoparticle aggregation. Model 4 shows gradual densification, rising from 0.40 g/cm³ to approximately 0.85 g/cm³ near 1500 mm, before stabilising around 0.80–0.82 g/cm³, reflecting delayed but substantial structural consolidation.

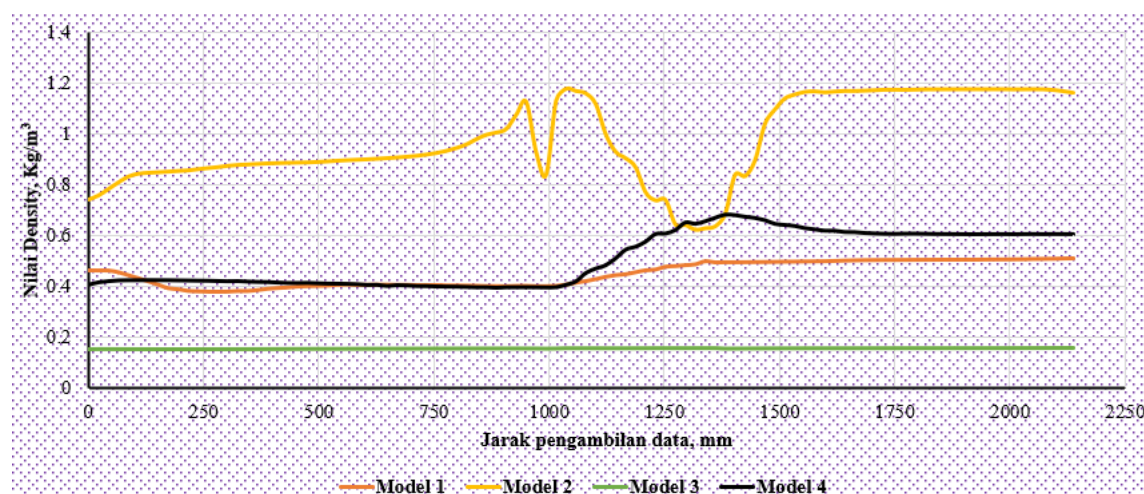


Fig. 2. Density Value Variation Along Data Acquisition Distance for Four Coating Models

These trends align with previous findings in nanoparticle-based coating research, where rapid density fluctuations are commonly associated with inconsistent particle dispersion or non-uniform deposition kinetics. Studies by Mohamed et al. reported that coatings with higher nanoparticle concentrations tend to exhibit density peaks when agglomeration occurs, followed by stabilisation once particle packing becomes uniform (Uniyal, Gaur, Yadav, Khan, & Ahmed, 2024). Similarly, Xu observed that density instability often indicates transitional phases during coating consolidation, especially when thermal or mechanical disturbances influence layer formation (Xu et al., 2025). The pronounced fluctuating pattern of Model 3 and the late-stage densification of Model 4 are consistent with these observations, suggesting that nanoparticle behaviour plays a crucial role in determining coating uniformity and long-term structural integrity.

The density variations illustrated in **Fig. 3** reveal distinct behavioural patterns among the four coating models over the 0–2250 mm measurement distance. Model 1 begins with a relatively high density of approximately 0.55 g/cm³, then gradually declines to about 0.48 g/cm³ near 250 mm, before increasing

steadily and stabilising at 0.58–0.60 g/cm³ after 1500 mm. Model 2 exhibits a contrasting trend, starting near 0.38 g/cm³ and decreasing progressively until a sharp drop occurs at around 1000 mm, where its density falls to approximately 0.20 g/cm³ before stabilising near 0.25–0.27 g/cm³. Model 3 shows minimal variation, maintaining density values between 0.15 and 0.18 g/cm³, reflecting consistent but low-quality coating uniformity. Model 4 starts at 0.35 g/cm³, experiences a moderate decline toward 0.30 g/cm³, and later stabilises near 0.32 g/cm³ beyond 1250 mm. These differences indicate that Models 1 and 4 achieve more stable long-range densification, whereas Models 2 and 3 display structural inconsistencies that may indicate insufficient nanoparticle bonding or early-layer compaction failure. These findings are consistent with previous studies reporting that nanoparticle-based coatings often exhibit density transitions influenced by particle concentration, thermal gradients, and deposition stability. Mohamed et al. demonstrated that coatings with well-dispersed nanoparticles tend to show gradual densification with distance, particularly when interparticle bonding strengthens during solidification (Diao, Jiang, Yang, Lu, & Zhu, 2024). Meanwhile, Xu observed that abrupt density drops, similar to those seen in Model 2, often occur due to nanoparticle agglomeration or disruption in the deposition flow, compromising coating integrity (Xu et al., 2025). The rebound and stabilising pattern of Model 1 aligns with earlier findings by researchers who noted that coatings with optimised nanoparticle ratios eventually reach a higher density equilibrium after initial fluctuations. Overall, the density behaviours represented in **Fig. 3** suggest varying levels of coating maturity among the models, with Model 1 demonstrating the most efficient structural consolidation.

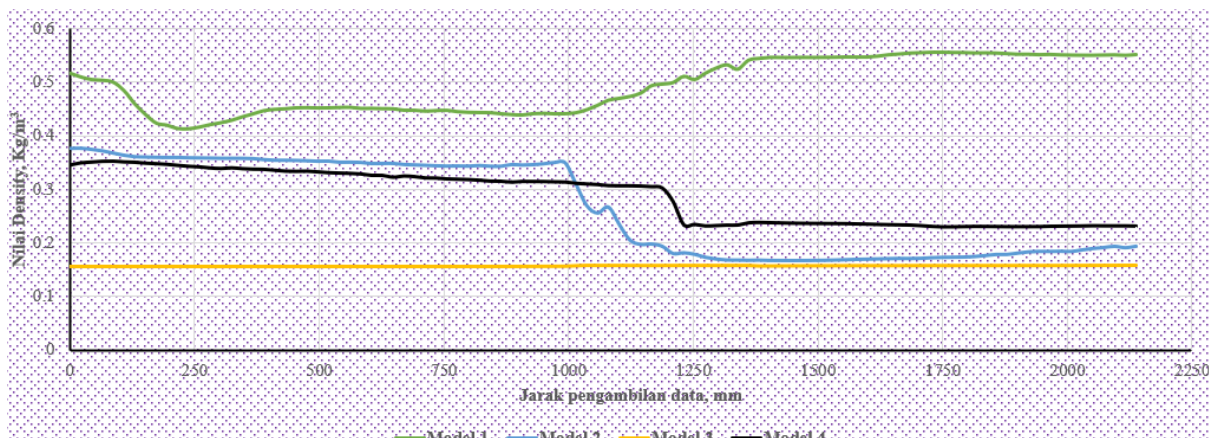


Fig. 3. Variation of Density Values Along Measurement Distance for Models 1–4

The friction value trends in **Fig. 4** highlight substantial differences in mechanical response among the four coating models along the 0–2250 mm measurement distance. Model 1 begins at approximately 600,000 N/m², briefly dips to around 500,000 N/m², and then gradually increases toward 700,000 N/m², indicating progressive surface interaction strengthening. Model 2 maintains the lowest friction values, ranging narrowly between 350,000 and 400,000 N/m², reflecting limited resistance likely due to poor interlayer bonding or insufficient coating hardness. Model 3 exhibits the highest initial friction value at around 1,350,000 N/m², which decreases sharply after 250 mm and stabilises near 850,000–900,000 N/m², suggesting that the coating undergoes early structural breakdown before reaching a more stable frictional state. Model 4 shows moderate friction levels, beginning at 600,000 N/m², rising gradually to 900,000 N/m², and stabilising around 950,000 N/m² beyond 1500 mm, indicating stronger interfacial adhesion than in Models 1 and 2. These observations suggest that Models 3 and 4 exhibit superior mechanical resistance, though Model 3 shows instability in the early region.

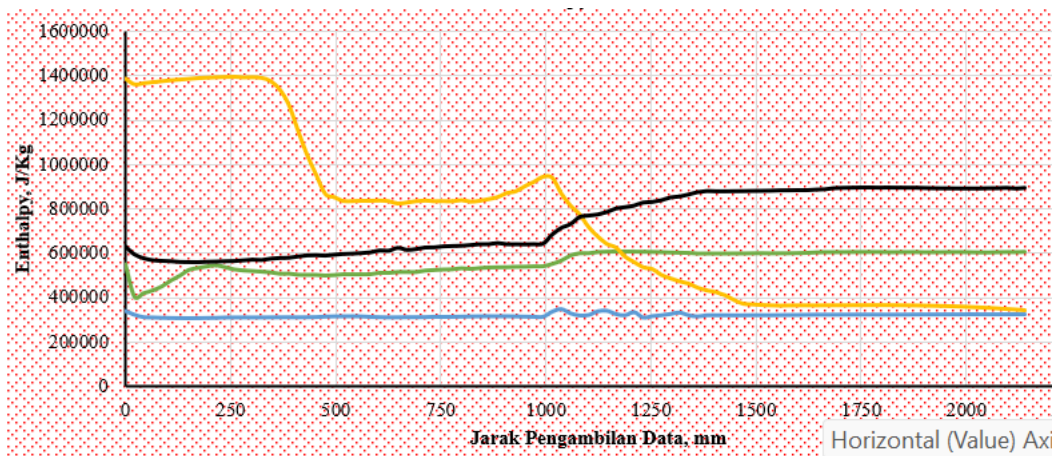


Fig. 4. Friction Value Variation Along Measurement Distance for Models 1–4

These friction behaviours align with previous research, which shows that nanoparticle-reinforced coatings tend to exhibit improved frictional performance due to enhanced hardness, surface compaction, and tribolayer formation. Mohamed et al. reported that coatings containing metal-oxide nanoparticles typically achieve friction reduction only after reaching structural equilibrium, following an initial period of instability similar to the transition seen in Model 3 (Diao et al., 2024). Meanwhile, Xu highlighted that coatings with poor nanoparticle dispersion often maintain low but unstable friction values due to weak interfacial bonding, which aligns with the consistently low friction performance of Model 2 (Xu et al., 2025). The gradual friction enhancement observed in Models 1 and 4 resembles patterns documented in earlier tribological studies, where coating densification over increasing distance promotes better load transfer and wear resistance. Overall, the friction trends in Fig. 4 reflect typical tribological responses of nanoparticle-modified coatings and provide insight into the varying mechanical robustness of the tested models.

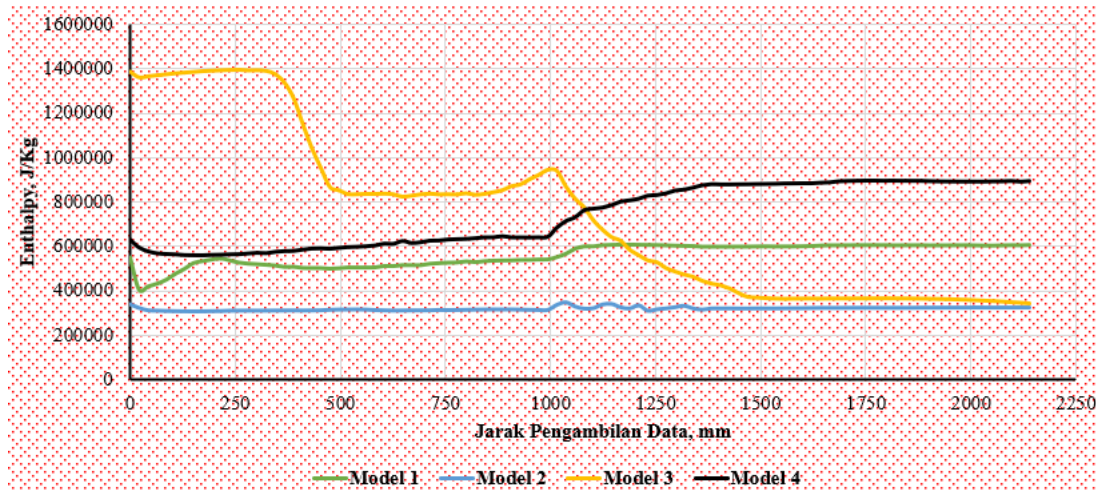


Fig. 5. Comparison of Friction Values Across Measurement Distance for Models 1–4

The friction profiles in Fig. 5 clearly demonstrate the comparative mechanical performance of the four coating models along the 0–2250 mm measurement distance. Model 1 exhibits moderate friction behaviour, starting at approximately 600,000 N/m², then dipping to 500,000 N/m², and eventually stabilising at 650,000–700,000 N/m², suggesting gradual surface hardening and consistent coating interaction. Model 2 exhibits the lowest and most stable friction values throughout the test, remaining within the narrow range of 350,000–380,000 N/m², indicating minimal resistance and potentially weaker coating adhesion or insufficient nanoparticle reinforcement. Model 3 displays the highest initial friction at around 1,350,000 N/m², followed by a significant reduction to 850,000 N/m² and later a

decline toward 450,000 N/m² beyond 1500 mm, reflecting significant structural degradation or a breakdown of the coating surface layer. Meanwhile, Model 4 shows steady improvement in friction resistance, beginning at approximately 600,000 N/m², rising sharply near the 1000 mm point to 900,000–950,000 N/m², and stabilising thereafter, indicating stronger load-bearing capacity and better interfacial bonding compared to Models 1 and 2.

These frictional behaviours correspond well with earlier studies on nanoparticle-enhanced coating systems, which demonstrate that friction stability and resistance are strongly influenced by nanoparticle dispersion, coating hardness, and tribolayer formation. Mohamed et al. observed that coatings with uneven nanoparticle distribution tend to exhibit sharp drops in frictional performance due to localised failure of the coating structure, a trend similar to the declining pattern observed in Model 3 (Diao et al., 2024). Xu further reported that coatings exhibiting consistently low friction, such as Model 2, typically possess weak cohesive strength and limited surface durability, making them prone to wear under prolonged sliding interaction (Xu et al., 2025). Conversely, the progressive improvement observed in Model 4 reflects mechanisms described in previous tribological analyses, in which nanoparticle-induced densification increases mechanical resistance and enhances interfacial load transfer over distance. Overall, the comparative friction values in **Fig. 5** indicate that while Models 1 and 4 demonstrate stronger long-term frictional stability, Model 3 experiences early mechanical breakdown, and Model 2 remains structurally weak despite its low friction response.

The present study offers several novel contributions to the understanding of nanoparticle-based coating performance, particularly through the combined analysis of density evolution and frictional behaviour along extended measurement distances, which has rarely been examined simultaneously in previous coating studies. Unlike earlier research that typically focuses on single-point measurements or short-range coating evaluations, this work provides a comprehensive longitudinal assessment across 2250 mm, revealing how coating stability, densification processes, and mechanical resistance evolve dynamically over distance. The identification of distinct behavioural signatures, such as the late-stage densification in Models 1 and 4, the sharp instability patterns in Models 2 and 3, and the tribological transitions observed at midpoint distances, offers a deeper understanding of coating formation mechanisms that has not been extensively documented in the coating literature.

Another key novelty lies in integrating density variation profiles with frictional response curves, enabling a more detailed correlation between microstructural consolidation and mechanical performance. For example, the study shows that coatings with stable density growth (such as Model 4) tend to exhibit improved frictional resistance at later stages, while those experiencing density collapse (such as Model 3) undergo significant mechanical degradation. This direct linkage provides new insight into the structure–property relationship in nanoparticle coatings, extending the findings of Diao et al. and Xu, who demonstrated that coating behaviour is not static but evolves dynamically depending on distance, deposition stability, and nanoparticle interaction mechanisms. Furthermore, the comparative evaluation of four distinct models makes an original contribution by identifying which coating formulations exhibit greater long-term robustness, thereby making the study valuable for future optimisation of advanced protective coating systems.

4. Conclusion

This study provides a comprehensive evaluation of four nanoparticle-based coating models by analysing their density evolution and frictional behaviour along an extended measurement distance of 2250 mm. The results demonstrate that each coating model exhibits distinct structural and mechanical characteristics, strongly influenced by nanoparticle dispersion, formulation properties, and consolidation behaviour. Model 1 and Model 4 showed favourable performance, with progressive densification and improved frictional stability at longer distances, indicating superior microstructural consolidation and mechanical resilience. In contrast, Model 2 maintained consistently low density and friction values, suggesting limited structural robustness, while Model 3 experienced pronounced instability, characterised by density collapse and frictional deterioration, reflecting inadequate coating integrity under extended mechanical interaction.

Correlation between density variation and frictional response revealed that coatings that achieved stable densification generally exhibited enhanced tribological resistance, whereas coatings with fluctuating or declining density exhibited mechanical degradation, supporting observations from previous nanoparticle coating studies. These findings highlight the importance of long-distance evaluation for assessing coating durability, as short-range measurements may miss the full spectrum of structural transitions. Overall, the study provides new insights into the dynamic behaviour of nanoparticle coatings and offers a comparative foundation for optimising formulation strategies to improve coating performance in demanding engineering environments. Future work should investigate the influence of environmental variables, nanoparticle morphology, and multi-layered architectures to refine coating reliability further and expand applicability across industrial sectors.

Acknowledgement

The authors would like to express their sincere appreciation for the collective support and collaboration that enabled the completion of this research. This work was fully funded by the personal contributions of all authors, reflecting their shared commitment to advancing scientific understanding in nanoparticle-based coating technologies. The authors also extend their gratitude to the laboratory staff and technical personnel who provided essential assistance during material preparation, experimental testing, and data analysis. Their contributions were invaluable to the successful execution of this study.

References

Alam, M. A., Samad, U. A., Anis, A., Alam, M., Ubaidullah, M., & Al-Zahrani, S. M. (2021). Effects of SiO₂ and ZnO nanoparticles on epoxy coatings and its performance investigation using thermal and nanoindentation technique. *Polymers*, 13(9), 1490.

Bahagia, B., Nizar, M., Yasin, M. H. M., Rosdi, S. M., & Faisal, M. (2025). Advancements in Communication and Information Technologies for Smart Energy Systems and Renewable Energy Transition: A Review. *International Journal of Engineering and Technology (IJET)*, 1(1), 1–29.

Bo, Z., Said, M. F. M., Erdiwan Syah, E., Mamat, R., & Xiaoxia, J. (2025). A review of oxygen generation through renewable hydrogen production. *Sustainable Chemistry for Climate Action*, 100079. Retrieved from <https://doi.org/https://doi.org/10.1016/j.scca.2025.100079>

Chauhan, H. R., Saladi, S., Variya, S., Solanki, A., Tailor, S., Sooraj, K. P., ... Joshi, S. (2023). Role of micro-and nano-CeO₂ reinforcements on characteristics and tribological performance of HVOF sprayed Cr₃C₂-NiCr coatings. *Surface and Coatings Technology*, 467, 129684.

Chen, Q., Xu, S., He, Y., Yan, S., Fan, Y., Li, Z., ... Gong, X. (2024). Enhancement of corrosion and wear resistance of Ni-P coatings stems from the synergistic effects of Cr₃C₂ and heat treatment. *Langmuir*, 40(31), 16400–16418.

Chopra, S., Banshiwal, J. K., Singh, A., & Bag, D. S. (2024). Sophisticated Characterization Techniques for Structure–Property Evaluation of Functional Coatings. *Functional Coatings: Innovations and Challenges*, 522–583.

Conradi, M., Kocijan, A., Kosec, T., & Podgornik, B. (2020). Manipulation of TiO₂ nanoparticle/polymer coatings wettability and friction in different environments. *Materials*, 13(7), 1702.

Diao, K., Jiang, Q., Yang, M., Lu, J., & Zhu, Y. (2024). Enhancing the dynamic thermal stability of metal oxide oil-based nanofluids through synchronous chemical modification and physical coating. *Surfaces and Interfaces*, 46, 104119.

Erdiwan Syah, Gani, A., Desvita, H., Mahidin, Bahagia, Mamat, R., & Rosdi, S. M. (2025). Investigation of heavy metal concentrations for biocoke by using ICP-OES. *Results in Engineering*, 25, 103717. Retrieved from <https://doi.org/https://doi.org/10.1016/j.rineng.2024.103717>

Erdiwan Syah, Gani, A., Desvita, H., Mahidin, Viena, V., Mamat, R., & Sardjono, R. E. (2024). Analysis study and experiments SEM-EDS of particles and porosity of empty fruit bunches. *Case Studies*

in *Chemical and Environmental Engineering*, 9, 100773. Retrieved from <https://doi.org/https://doi.org/10.1016/j.cscee.2024.100773>

Erdiwansyah, Gani, A., Desvita, H., Mamat, R., & Ghazali, M. F. (2025). Analysis of the calorific value of biocoke from empty fruit bunches with temperature variations and FTIR characterisation. *Energy Storage and Saving*. Retrieved from <https://doi.org/https://doi.org/10.1016/j.enss.2025.03.006>

Erdiwansyah, Gani, A., Mamat, R., Bahagia, Nizar, M., Yana, S., ... Rosdi, S. M. (2024). Prospects for renewable energy sources from biomass waste in Indonesia. *Case Studies in Chemical and Environmental Engineering*, 10, 100880. Retrieved from <https://doi.org/https://doi.org/10.1016/j.cscee.2024.100880>

Erdiwansyah, Gani, A., Zaki, M., Mamat, R., Nizar, M., Rosdi, S. M., ... Sarjono, R. E. (2023). Analysis of technological developments and potential of biomass gasification as a viable industrial process: A review. *Case Studies in Chemical and Environmental Engineering*, 8, 100439. Retrieved from <https://doi.org/https://doi.org/10.1016/j.cscee.2023.100439>

Erdiwansyah, Mahidin, Husin, H., Nasaruddin, Gani, A., & Mamat, R. (2023). Modification of perforated plate in fluidized-bed combustor chamber through computational fluid dynamics simulation. *Results in Engineering*, 19, 101246. Retrieved from <https://doi.org/https://doi.org/10.1016/j.rineng.2023.101246>

Erdiwansyah, Mamat, R., Basrawi, F., Syafrizal, Ghazali, M. F., & Rosdi, S. M. (2025). Advancing local algae biorefineries through waste integration and industry 4.0 for sustainable bioenergy production. *Total Environment Engineering*, 4, 100037. Retrieved from <https://doi.org/https://doi.org/10.1016/j.teengi.2025.100037>

Erdiwansyah, Mamat, R., Ghazali, M. F., Basrawi, F., Rosdi, S. M., & Bahagia. (2025). A recent review of alternative fuels in SI engines: Performance, emissions, and combustion aspects. *Next Research*, 2(4), 100810. Retrieved from <https://doi.org/https://doi.org/10.1016/j.nexres.2025.100810>

Erdiwansyah, Mamat, R., Rosdi, S. M., Ghazali, M. F., Rashid, M. I. M., Syahir, A. Z., ... Tamimi, A. (2026). A review on AI-enhanced circular energy storage systems for renewable integration. *Energy* 360, 5, 100051. Retrieved from <https://doi.org/https://doi.org/10.1016/j.energ.2025.100051>

Erdiwansyah, Mamat, R., Sani, M. S. M., & Sudhakar, K. (2019). Renewable energy in Southeast Asia: Policies and recommendations. *Science of The Total Environment*. Retrieved from <https://doi.org/https://doi.org/10.1016/j.scitotenv.2019.03.273>

Erdiwansyah, Mamat, R., Syafrizal, Ghazali, M. F., Basrawi, F., & Rosdi, S. M. (2025). Emerging Role of Generative AI in Renewable Energy Forecasting and System Optimization. *Sustainable Chemistry for Climate Action*, 100099. Retrieved from <https://doi.org/https://doi.org/10.1016/j.scca.2025.100099>

Ezzeddin, B., & Al-khalidi, M. T. A. (2024). An investigation into the effect of using different metal oxide nanoparticles on the anti-corrosion properties of coatings: a comparative study. *Moroccan Journal of Chemistry*, 12(2), 657–675.

Gani, A., Adisalamun, Arkan D, M. R., Suhendrayatna, Reza, M., Erdiwansyah, ... Desvita, H. (2023). Proximate and ultimate analysis of corncob biomass waste as raw material for biocoke fuel production. *Case Studies in Chemical and Environmental Engineering*, 8, 100525. Retrieved from <https://doi.org/https://doi.org/10.1016/j.cscee.2023.100525>

Gani, A., Erdiwansyah, Desvita, H., Mamat, R., Ghazali, M. F., Ichwansyah, F., & Naim, A. (2025). Thermochemical Characterization of Cassava Peel Biocoke for Renewable Energy at Varying Pyrolysis Temperatures. *Results in Engineering*, 105159. Retrieved from <https://doi.org/https://doi.org/10.1016/j.rineng.2025.105159>

Gani, A., Erdiwansyah, Desvita, H., Meilina, H., Fuady, M., Hafist, M., ... Mahidin. (2024). Analysis of chemical compounds and energy value for biocoke fuel by FTIR and TGA. *Case Studies in Chemical and Environmental Engineering*, 100644. Retrieved from <https://doi.org/https://doi.org/10.1016/j.cscee.2024.100644>

Gani, A., Erdiwansyah, Desvita, H., Munawar, E., Mamat, R., Nizar, M., ... Sarjono, R. E. (2024).

Comparative analysis of HHV and LHV values of biocoke fuel from palm oil mill solid waste. *Case Studies in Chemical and Environmental Engineering*, 9, 100581. Retrieved from <https://doi.org/https://doi.org/10.1016/j.cscee.2023.100581>

Gani, A., Erdiwansyah, Desvita, H., Saisa, Mahidin, Mamat, R., ... Sarjono, R. E. (2024). Correlation between hardness and SEM-EDS characterization of palm oil waste based biocoke. *Energy Geoscience*, 100337. Retrieved from <https://doi.org/https://doi.org/10.1016/j.engeos.2024.100337>

Gani, A., Erdiwansyah, Munawar, E., Mahidin, Mamat, R., & Rosdi, S. M. (2023). Investigation of the potential biomass waste source for biocoke production in Indonesia: A review. *Energy Reports*, 10, 2417–2438. Retrieved from <https://doi.org/https://doi.org/10.1016/j.egyr.2023.09.065>

Gani, A., Mahidin, Faisal, M., Erdiwansyah, Desvita, H., Kinan, M. A., ... Mamat, R. (2024). Analysis of combustion characteristics and chemical properties for biocoke fuel. *Energy Geoscience*, 5(4), 100331. Retrieved from <https://doi.org/https://doi.org/10.1016/j.engeos.2024.100331>

Gani, A., Saisa, S., Muhtadin, M., Bahagia, B., Erdiwansyah, E., & Lisafitri, Y. (2025). Optimisation of home grid-connected photovoltaic systems: performance analysis and energy implications. *International Journal of Engineering and Technology (IJET)*, 1(1), 63–74.

Iqbal, Erdiwansyah, Faisal, M., Mahyuddin, Muhtadin, Ghazali, M. F., & Mamat, R. (2025). Thermal Performance and Flue Gas Emission Analysis of Biomass Combustion Chamber for Small-Scale Brick Production. *Sustainable Chemistry for Climate Action*, 100169. Retrieved from <https://doi.org/https://doi.org/10.1016/j.scca.2025.100169>

Kaya, E., & Ulutan, M. (2022). Tribomechanical and microstructural properties of cathodic arc-deposited ternary nitride coatings. *Ceramics International*, 48(15), 21305–21316.

Liang, Z., & Rabkin, E. (2024). Compressive strength of the Cu-Au nanoparticles fabricated by solid state dewetting. In #PLACEHOLDER_PARENT_METADATA_VALUE#.

Louis, S., Arukula, R., Yang, D., Kim, T., Wu, X., & Qi, X. (2026). Effects of dispersion methods on dynamic and thermal mechanical properties of GNP–epoxy nanocomposite coatings. *Progress in Organic Coatings*, 210, 109652.

Mahidin, M., Hamdani, H., Hisbullah, H., Erdiwansyah, E., Muhtadin, M., Faisal, M., ... Sidik, N. A. C. (2022). Experimental study on the FBC chamber for analysis of temperature and combustion efficiency using palm oil biomass fuel. *Transactions of the Canadian Society for Mechanical Engineering*, 46(3), 639–649.

Mamat, R., Erdiwansyah, Ghazali, M. F., Rosdi, S. M., Syafrizal, & Bahagia. (2025). Strategic framework for overcoming barriers in renewable energy transition: A multi-dimensional review. *Next Energy*, 9, 100414. Retrieved from <https://doi.org/https://doi.org/10.1016/j.nxener.2025.100414>

Mamat, R., Ghazali, M. F., Erdiwansyah, & Rosdi, S. M. (2025). Potential of renewable energy technologies for rural electrification in Southeast Asia: A review. *Cleaner Energy Systems*, 12, 100207. Retrieved from <https://doi.org/https://doi.org/10.1016/j.cles.2025.100207>

Mani, M., Thiyyagu, M., Afriyie Mensah, R., Das, O., & Shanmugam, V. (2024). Nano-enhanced epoxy sandwich composites: Investigating mechanical properties for future aircraft construction. *Polymers for Advanced Technologies*, 35(6), e6492.

Muhibbuddin, Erdiwansyah, Syahir, A. Z., Mamat, R., & Sardjono, R. E. (2025). A review of optimization strategies for hybrid renewable energy systems toward sustainable clean energy. *Results in Engineering*, 28, 108363. Retrieved from <https://doi.org/https://doi.org/10.1016/j.rineng.2025.108363>

Nizar, M., Yana, S., Bahagia, Erdiwansyah, Mamat, R., & Viena, V. (2025). Bibliometric analysis of global research on organic waste enzymes for plastic biodegradation: Trends, microbial roles, and process optimization. *Cleaner and Circular Bioeconomy*, 12, 100164. Retrieved from <https://doi.org/https://doi.org/10.1016/j.clcb.2025.100164>

Pan, W., Han, Y., Wang, Z., Wang, C., Zhang, C., Zhu, P., ... Qin, Z. (2023). Degradation mechanisms of polyurethane grouting materials under quasi-static and cyclic compression loading: density and size effects. *Construction and Building Materials*, 408, 133795.

Pang, B., Yang, T., Wu, Z., Li, Z., Jin, Z., Zhang, W., ... Gan, Y. (2024). Li5. 5PS4. 5Cl1. 5-Based All-

Solid-State Battery with a Silver Nanoparticle-Modified Graphite Anode for Improved Resistance to Overcharging and Increased Energy Density. *ACS Applied Materials & Interfaces*, 16(16), 20510–20519.

Patidar, S., Tiwari, J. K., Das, A., Sathish, N., Mishra, S., Ashiq, M., & Srivastava, A. K. (2024). Study on microstructure and tribological behavior of additively manufactured graphene/AlSi10Mg composite. *Journal of Materials Engineering and Performance*, 33(22), 12503–12516.

Pownraj, C., & Valan Arasu, A. (2021). Effect of dispersing single and hybrid nanoparticles on tribological, thermo-physical, and stability characteristics of lubricants: a review. *Journal of Thermal Analysis & Calorimetry*, 143(2).

Pradhan, N. C., Sahoo, P. K., Kushwaha, D. K., Mani, I., Srivastava, A., Sagar, A., ... Makwana, Y. (2021). A novel approach for development and evaluation of LiDAR navigated electronic maize seeding system using check row quality index. *Sensors*, 21(17), 5934.

Uglov, V. V., Kuleshov, A. K., Rusalsky, D. P., Samzov, M. P., & Dementshenok, A. N. (2002). Friction coefficient, microstructure and thermal stability of amorphous aC coatings. *Surface and Coatings Technology*, 158, 699–703.

Uniyal, P., Gaur, P., Yadav, J., Khan, T., & Ahmed, O. S. (2024). A review on the effect of metal oxide nanoparticles on tribological properties of biolubricants. *Acs Omega*, 9(11), 12436–12456.

Xu, M., Ali, S., Kurniawan, R., Gautam, R. K. S., Sundaresan, T. K., & Ahmad, K. (2025). Nanoparticle-based lubrication during machining: Synthesis, application, and future scope—A critical review. *The International Journal of Advanced Manufacturing Technology*, 136(10), 4141–4174.